

## RESEARCH ARTICLE

# The Insulation Performance of Novel Refrigerant Gas as an Alternative to SF<sub>6</sub> for Medium Voltage Switchgear

RIZWAN AHMED<sup>1</sup>, RAHISHAM ABD-RAHMAN<sup>1</sup>, (Member, IEEE),  
ZAHID ULLAH<sup>2,3</sup>, (Graduate Student Member, IEEE), RAHMAT ULLAH<sup>4</sup>, IRFAN SAMI<sup>5</sup>,  
AND MOHD FAIROUZ MOHD YOUSOF<sup>1</sup>, (Member, IEEE)

<sup>1</sup>Faculty of Electrical and Electronic Engineering, University Tun Hussein Onn Malaysia, Batu Pahat 86400, Malaysia

<sup>2</sup>Dipartimento di Elettronica, Informazione e Bioingegneria, Politecnico di Milano, 20133 Milan, Italy

<sup>3</sup>Department of Electrical Engineering, University of Management and Technology Lahore, Sialkot Campus, Sialkot 51310, Pakistan

<sup>4</sup>Advanced High Voltage Engineering Research Centre, School of Engineering, Cardiff University, CF10 3AT Cardiff, U.K.

<sup>5</sup>Research and Development Department, Milim Syscon Company Ltd., Seongnam 13207, South Korea

Corresponding author: Zahid Ullah (Zahid.ullah@polimi.it)

This work was supported in part by the University Tun Hussein Onn Malaysia under Grant FRGS-K301, and in part by Politecnico di Milano for providing Open Access within the CRUI CARE Agreement.

**ABSTRACT** Gas-insulated systems are widely utilized in the electric power sector to transmit and distribute electrical energy. Sulphur-hexafluoride (SF<sub>6</sub>) has dominated gas insulation in high-voltage insulation technology since the early 60s. It is a greenhouse gas with a protracted lifespan in the atmosphere. This paper proposes an economical and comparatively more environmentally friendly R507 gas alternative to SF<sub>6</sub> for medium-voltage applications. R507 has been analyzed experimentally through power frequency breakdown and lightning impulse testing to validate the performance and theoretical concepts. R507 has a very low liquefaction temperature of  $-46.7^{\circ}\text{C}$ , but it must still be mixed with buffer gases such as CO<sub>2</sub>, N<sub>2</sub>, or dry air to meet the diverse liquefaction temperature applications. Various field utilization factors under AC and lightning impulse voltages are used in the experiments, along with different electrode geometries, including sphere-to-plane and rod-to-plane (i.e., quasi-homogeneous and inhomogeneous electric field distribution). For comparison, identical experiments are conducted with pure SF<sub>6</sub>. R507 gas was found to be a promising substitute for SF<sub>6</sub> gas, with its dielectric strength being approximately 0.95 times that of SF<sub>6</sub> gas. A positive synergistic effect is present between R507 and CO<sub>2</sub>, along with the good self-recoverability property of the gas mixture. The current research study serves as a fundamental resource for characterizing the R507/CO<sub>2</sub> gas mixture insulation properties to be utilized in practical applications.

**INDEX TERMS** Global warming potential, SF<sub>6</sub>, insulation, refrigerants, lightning impulses.

## I. INTRODUCTION

In high-voltage insulation, gas-insulated equipment (GIE), including gas-insulated transmission lines (GIL), gas-insulated switchgear (GIS), and gas-insulated transformers (GIT), have been utilized for different voltage levels due to their advantages of high reliability, efficiency, and long maintenance cycle. Sulfur hexafluoride (SF<sub>6</sub>), a synthetic gas,

The associate editor coordinating the review of this manuscript and approving it for publication was Ali Raza<sup>1</sup>.

has been utilized in GIE owing to its good insulation and arc-quenching properties. With a global warming potential (GWP) of 25,200 and an atmospheric lifespan of 3,200 years, SF<sub>6</sub> is one of the most potent greenhouse gases [1], [2], [3]. The key contributor to the greenhouse gas emission (GHG) in electrical power systems is SF<sub>6</sub> gas, of which 1 kg release is equivalent to 25.2 tons of carbon dioxide (CO<sub>2</sub>) due to its high GWP [4], [5], [6]. Additionally, the atmospheric concentration of SF<sub>6</sub> varies from 3.67 parts per trillion (ppt) in 1994 to 10.41 ppt in 2020, showing a tendency of 10%

annual growth in emissions [7], [8]. Therefore, much research has been performed to find a substitute for SF<sub>6</sub> as a dielectric gas in GIE.

Recent studies show that reducing SF<sub>6</sub> emissions requires completely shifting to SF<sub>6</sub>-free technology. The ever-growing installed base and the banked quantity of SF<sub>6</sub> would lead to gradually rising SF<sub>6</sub> emissions (nearly doubling today's emissions in the next 80 years), even with the exclusive employment of the most sophisticated technologies with minimal emissions [9], [10], [11], [12]. Therefore, the legal frameworks need to be quickly adjusted and established to assist and secure a complete transition as quickly as is technically and economically feasible.

The primary concern about alternative gases is ensuring that their insulation properties are equivalent to or superior to those of SF<sub>6</sub>. Identifying and optimizing alternative gases necessitates significant research and development [13]. The quest for substitute gases represents a crucial stride toward realizing a sustainable energy prospect. Substituting SF<sub>6</sub> with alternative gases can reduce the ecological footprint of high-voltage applications and positively contribute to climate change amelioration [14], [15]. Conventional gases such as dry air, nitrogen, carbon dioxide, or mixtures exhibit a lower global warming potential than SF<sub>6</sub>, but their dielectric strength is limited to only 40% or less [16]. Incorporating a buffer gas as an insulating or current-interrupting medium would necessitate substantial modifications to the configuration of high-voltage equipment. These modifications could include augmenting the filling pressure or equipment dimensions by a minimum of 2.5 times. Excessive elevation in pressure can potentially jeopardize the power system's safety and stability [17].

The main requirements for a specific gas or gas mixture used in high voltage insulation applications are high dielectric strength, low condensation temperature, thermal stability, minimal environmental impact, low toxicity, chemical inertness with other constituent materials of the apparatus, non-flammability, availability, and moderate cost [18]. Table 1 lists the disadvantages of dielectric gases as an alternative to SF<sub>6</sub>.

Refrigerant gases have been acknowledged as feasible alternatives to SF<sub>6</sub> in high and medium-voltage applications owing to their comparatively lower GWP than SF<sub>6</sub> and convenient availability. R410A [19], R12 [20], R134 [21], R1234yf [22], R1234ze(E) [23], and R32 [24] are commonly employed refrigerant gases. Refrigerant gases demonstrate advantageous insulating characteristics and possess dielectric strength equivalent to or superior to SF<sub>6</sub>. Furthermore, their remarkable ability to extinguish electric arcs makes them suitable for utilization in high-voltage applications [24].

Nevertheless, utilizing refrigerant gases as a substitute for SF<sub>6</sub> presents certain obstacles. One of the primary obstacles pertains to the flammability of refrigerant gases, which could compromise safety if not appropriately managed. Moreover, certain types of refrigerant gases exhibit high costs and may

**TABLE 1. Comparison of SF<sub>6</sub> substitute gases.**

Quantity	Conversion from Gaussian and CGS EMU to SI <sup>a</sup>
Dry air, nitrogen, and carbon dioxide	Significant increase in pressure (>7 bar), Significant growth in equipment size, significant drop in withstand voltages in the event of flaws and imperfections.
Perfluorocarbons (CF <sub>4</sub> , C <sub>2</sub> F <sub>6</sub> , C <sub>3</sub> F <sub>8</sub> and <i>c</i> -C <sub>4</sub> F <sub>8</sub> )	Strong greenhouse gases, Low liquefaction temperature.
Mixtures of tri-fluorinated ketones (C <sub>5</sub> F <sub>10</sub> O, C <sub>6</sub> F <sub>12</sub> O/ technical air or CO <sub>2</sub> , CF <sub>3</sub> I)	Higher minimum operating temperature than SF <sub>6</sub> , classified as carcinogenic, mutagenic, and reproductively harmful.
Hydrofluoro-Olefins HFO-1234ze(E), HFO-1336mzz(E)	Acute toxicity, low boiling point, can be employed to MV GIE, operating temperature greater than SF <sub>6</sub> as pure (Limited to -15°C)
HFO 1234zeE	The spark voltages cause carbon dust to accumulate on the electrodes. Operating temperature greater than SF <sub>6</sub> as pure (Limited to -15°C)

not be economically viable for all high-voltage implementations [25].

This paper presents an investigation of the dielectric properties of a novel gas medium. To our knowledge, no study has been published on the insulation strength of R507 gas until now. This study analyzes the fundamental dielectric properties of R507 gas mixtures with CO<sub>2</sub>/N<sub>2</sub> under varying pressure, air gaps, and electric field configurations. R507 is predominantly employed as a refrigerant gas; however, it has been subject to investigation as a prospective substitute for SF<sub>6</sub> in gas dielectrics for medium-voltage applications. The present context highlights several benefits of employing R507 as a dielectric gas. R507 has a GWP of 3985, much lower than SF<sub>6</sub> (25,200). This indicates a significant reduction in the discharge of greenhouse gases. R507 is a safe alternative to SF<sub>6</sub> due to its non-toxic and non-flammable properties. It is cost-effective and readily available in every country and can potentially mitigate the system's total cost, particularly when retrofitting pre-existing systems. The proposed gas is compatible with pre-existing refrigeration and air conditioning systems. The basic physiochemical properties of R507 gas are presented in Table 2. R507 is a blend of two refrigerant gases, R125 and R143a gas; it is conventionally treated as a singular gas entity in practical applications due to the uniformity of its constituent proportions. Mardolcar et al. [26] performed a density function theory analysis on different refrigerant gases based on their polarization and relative permittivity and analyzed R507 as a potential dielectric gas. The chemical composition and molecular structure of R507 components can be seen in Table 3. The liquefaction temperature graph of R507 can be seen in Figure 1.

## II. EXPERIMENTAL SETUP AND PROCEDURE

### A. TEST PLATFORM

The dielectric breakdown strength of R507 and its mixture was examined under HVAC and Impulse voltage conditions,

**TABLE 2. Comparison of physical and chemical properties of R507 with SF<sub>6</sub> and CO<sub>2</sub>/N<sub>2</sub>.**

Property	R507	SF <sub>6</sub>	CO <sub>2</sub>	N <sub>2</sub>
Chemical formula	C <sub>2</sub> HF <sub>5</sub> /C <sub>3</sub> H <sub>2</sub> F <sub>6</sub>	SF <sub>6</sub>	CO <sub>2</sub>	N <sub>2</sub>
Molecular weight	98.86 g/mol	146.06 g/mol	44.01 g/mol	28.02 g/mol
Boiling point	-46.7 °C	-64 °C	-78.5 °C	-195.8 °C
Critical temperature	70.9 °C	45.5 °C	31.1 °C	-146.9 °C
Critical pressure	3.79 MPa	3.77 MPa	7.38 MPa	3.35 MPa
GWP	3985	23500	1	265-298
ODP	0	0	0	0
Flammability	None	None	None	None
Toxicity	Low toxicity	Moderate toxicity	None	None
Odor	Odorless	Odorless	Odorless	Odorless
Color	Colorless	Colorless	Colorless	Colorless

**TABLE 3. Composition of R507.**

Components (CAS-No)	Weight	Chemical structure
R-125 (354-33-6)	50%	$\begin{array}{c} \text{F} \quad \text{F} \\   \quad   \\ \text{H}-\text{C}-\text{C}-\text{F} \\   \quad   \\ \text{F} \quad \text{F} \end{array}$
R-143a (420-46-2)	50%	$\begin{array}{c} \text{F} \quad \text{H} \\   \quad   \\ \text{F}-\text{C}-\text{C}-\text{H} \\   \quad   \\ \text{F} \quad \text{H} \end{array}$

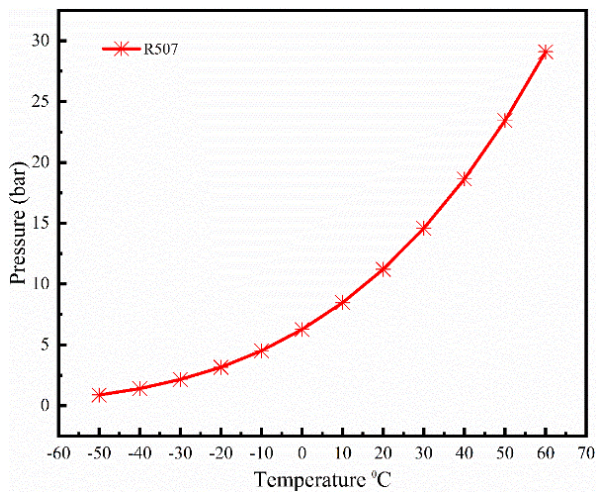


**FIGURE 1. Liquefaction temperature versus pressure curve of R507.**

following the ASTM D2477-07 and IEC60270 standard, while keeping laboratory atmospheric conditions constant (temperature  $t_0 = 20$  C, pressure  $p_0 = 0.1013$  MPa, absolute humidity  $h_0 = 11$  gm/m<sup>3</sup>) [27], [28]. The experimental investigations utilized the TERCO test configuration to produce the requisite test voltages. The test vessel was modified by

installing a linear actuator at its bottom layer to fulfill the technical necessity of adjusting the electrode gap length. The vessel was fabricated utilizing aluminum as its primary material, while its viewport was made of Plexiglas. The test vessel possessed a vertical dimension of 56 cm, a horizontal dimension of 120 cm, and a wall thickness of 5mm. These dimensions yielded a test gas volume of approximately 5.2 liters and a pressure-bearing capacity of 0.6 MPa. Pressure and vacuum gauges were installed to ensure precise gas pressure within the vessel.

The R507 liquefaction temperature is higher than CO<sub>2</sub> and N<sub>2</sub>. Gas mixing is done following Dalton’s law of partial pressure, as seen in Equation 1. According to the law, the partial pressure of the individual gases is equal to the sum of individual component gases.

$$P_T = \sum_{i=1}^n P_i \tag{1}$$

Here  $P_T$  is the total pressure inside the pressure vessel, where  $P_i$  is the partial pressure of individual component gas. The saturated vapor pressure under different liquefaction temperatures is shown in Figure 1.

**B. EXPERIMENTAL PROCEDURE**

The test procedure involved evacuating the test chamber to a pressure of 100 kPa using a vacuum pump and introducing CO<sub>2</sub>. The process was iterated five times to ensure the absence of contaminants within the pressurized vessel. A standing time of 24 hours is allotted to ensure the uniformity of the gas mixture. Furthermore, a unidirectional air valve was installed at the lower flange to facilitate the inlet and outlet of gas from the container.

The utilization of two distinct electrode configurations, namely sphere-plane, and point-plane, is employed to generate quasi-uniform and non-uniform electric fields. The quasi-uniform electric field dominating the GIL and GIS coaxial structure led to the selection of electrode configuration. To maintain clean electrodes, they undergo a cleaning process involving anhydrous alcohol and subsequent drying with cotton to eliminate dust particles. To achieve a surface roughness of less than 2.5 μm, the electrodes undergo a polishing process utilizing 5000 mesh sandpaper. Furthermore, three aging tests are performed on the test electrode arrangement before each test to eliminate any protrusions and minuscule particles on the electrodes.

A three-minute interval between two consecutive breakdown occurrences is established to accommodate the insulation self-recovery. A gradual increment in voltage is employed to prevent the statistical time lag-induced overestimation of electric strength, albeit at the cost of prolonging the experimental duration.

Consequently, it is common practice to employ a rapid voltage ramping rate of approximately 80% to 90% of the anticipated breakdown voltage, succeeded by incremental voltage augmentations of 0.5kV/s relative to the initial breakdown threshold. At least ten iterations of testing are conducted for

each test condition. In cases where the discrepancy between the initial and successive breakdown voltage exceeds 10%, the test is repeated, and the mean value of the test is documented as the breakdown voltage. Pure SF<sub>6</sub> gas is utilized for conducting benchmark tests.

The dimensions and shape of electrodes are configured to cover the electric field ranging from quasi-uniform to nonuniform. The field utilization factor,  $\eta$ , for each electrode configuration, is calculated using equation 2.

$$\eta = \frac{E_{mean}}{E_{max}} \tag{2}$$

where  $E_{max}$  is the maximum electric field of the electrode measured with the finite element method. Figures 2 and 3 show a typical example of simulation and computed electric field utilization factor for electrode geometries under consideration. The mean electric field  $E_{mean}$  is given by equation 3.

$$E_{mean} = \frac{v}{d} \tag{3}$$

Here  $v$  denotes the applied voltage, and  $d$  is the electrode gap. The calculated electric field utilization factor,  $\eta$ , for two electrode geometries at different air gaps are shown in Table 4.

TABLE 4. Simulated electric field utilization factor.

Electrode gap separation(mm)	5	10	15	20
Point-plane	0.10	0.06	0.04	0.03
Sphere-plane	0.78	0.63	0.53	0.46

C. TEST SETUP

A test transformer, a protection resistor, and a capacitive voltage divider make up the HVAC experimental circuit. The output voltage of the AC test transformer is 100 kV for single-stage operation and 200 kV for two-stage operation. A resistor is connected in series to protect the test transformer from damage during HVAC breakdown. A control desk with a peak, impulse, and DC voltmeter regulates the supply voltage to operate and control the Impulse and HVAC equipment. Using a measuring capacitor, the voltmeter determines the breakdown voltage in real time, as seen in Figure 4(a). The lightning impulse (LI) voltage experimental setup of 1/50 $\mu$ s wave is shown in Figure 4(b). The impulse waveform is generated by applying the DC charging voltage specified for the gap, and then the resistors at the wave tail and front produce the wave. A low-voltage divider unit is used to determine the voltage. The LI test 50% breakdown characteristics of the gas mixture were determined using the up-and-down method.

The dielectric strength of the R507 gas mixture is analyzed in this research using the 50 % breakdown voltage (U50 %) under a standard lightning impulse, which was

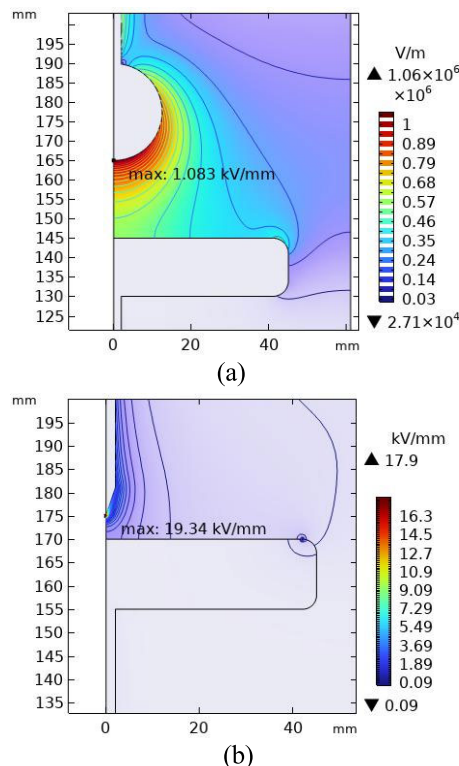


FIGURE 2. E<sub>max</sub> simulation for electrode configuration with (a) Sphere-plane and (b) Point-plane.

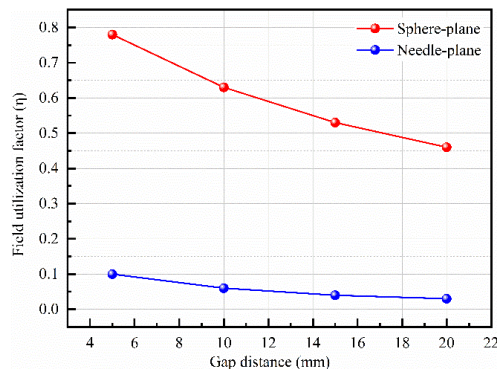


FIGURE 3. Electric field utilization factor at different gap distances.

determined using the up and down technique per the International Electro-Technical Commission (IEC) 60060-1 [20]. U50 % was calculated from at least 30 repetitions of valid test results [19]. Considering the insulation self-recovery time and space charge phenomena, a specific time interval is required between two consecutive shots. When the relaxation time between consecutive tests is maintained at 1 minute, an illustration of an up-and-down approach under the U50% test shows a large deviation from the mean value, as shown in Figure 5(a). The variation is reduced while maintaining the relaxation time of 5 minutes, and the standard deviation (SD) value is minimized, as seen in Figure 5(b). A fresh gas mixture and experimental electrodes were used for each test to guarantee the data’s accuracy.



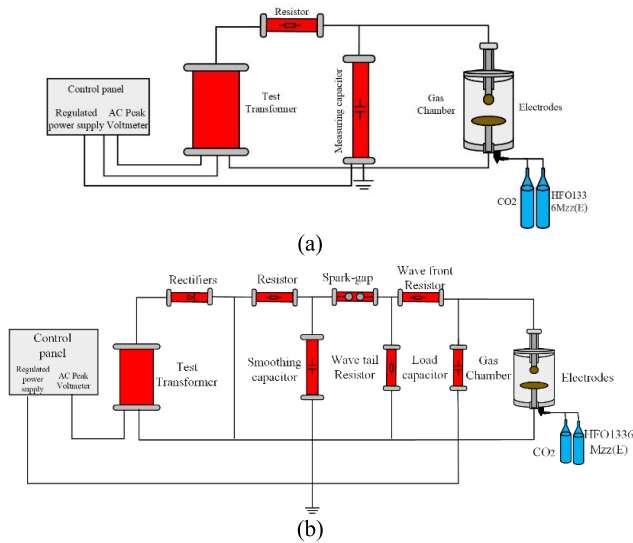


FIGURE 4. Schematic diagram of (a) AC and (b) Impulse voltage test circuit.

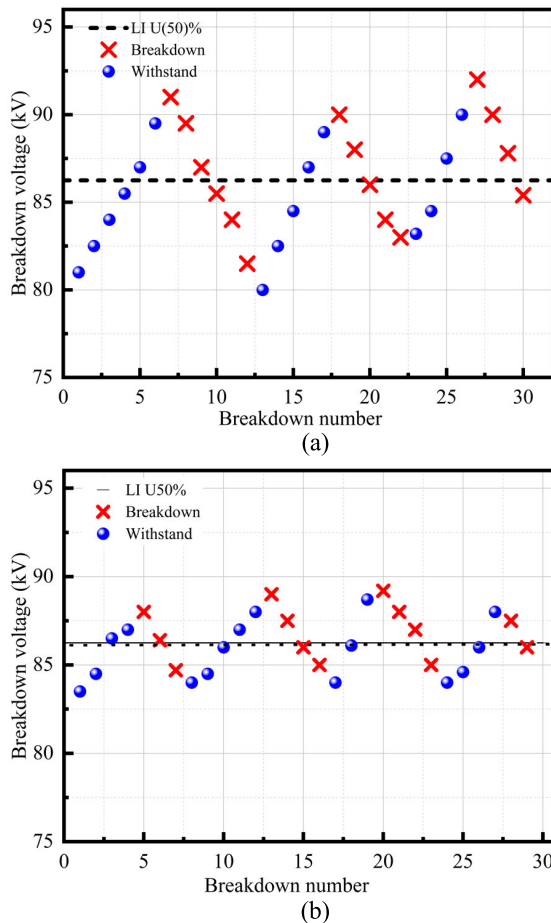


FIGURE 5. LI 50% breakdown testing example at 150 kPa with a time lag of (a) 1 minute and (b) 5 minutes.

### III. EXPERIMENTAL RESULTS

In this section, experimental results are discussed and presented. First, the proposed gas insulation strength is

compared to SF<sub>6</sub> under quasi-uniform and highly non-uniform fields for varying pressure and gap length. The experiments use varying HVAC air gaps and pressure for LI voltages. Then, the proposed gas mixture with CO<sub>2</sub> and N<sub>2</sub> is tested and analyzed under different electrode configurations and applied voltage test setups. The main objective is to determine the optimal mixture composition of R507 with CO<sub>2</sub>/N<sub>2</sub> for industrial applications that can substitute SF<sub>6</sub>.

#### A. INFLUENCE OF FIELD UNIFORMITY ON ELECTRICAL STRENGTH

Inherently, gases function perfectly as insulators. Nonetheless, ionization occurs using an electric field generated by certain free ions, and electrons gain sufficient energy through the collision. The symbol ‘ $\alpha$ ’ represents Townsend’s initial ionization coefficient, which denotes the number of electrons generated during the one-centimeter travel of an electron in an electric field.

R507 is a solid electronegative gas with a significant attraction for free electrons; detachment produces positive ions, while electron-neutral atom binding produces negative ions. Equation 4 indicates that the coefficient of detachment is represented by  $\gamma$ .

$$dN = N(\alpha - \gamma) dx \tag{4}$$

The distance traversed by each electron is denoted by  $dN$  in Equation 4, whereas the initial quantity of electrons is denoted by  $N$ . An exponential increase is observed in gas breakdown when  $\alpha > \gamma$  condition is met.

#### B. HVAC BREAKDOWN VOLTAGE OF R507 GAS MIXTURES AT UNIFORM PRESSURE

This study examines the effects of altering the pressure and mixture ratio of R507 gas and CO<sub>2</sub>/N<sub>2</sub> in sphere-plane and point-plane configurations on the properties of power frequency breakdown. In adherence to the guidelines outlined in ASTM D2477-07 and the IEC60270 standard for medium voltage applications [27], [28]. The analysis aims to determine how changing the mixture ratio affected the insulation characteristics of R507 gas and the variation of air gaps.

The breakdown voltage rises with increasing electrode separation distance and vice versa. This is because balancing the electric field between the high voltage and ground electrodes requires a greater field potential. Hence, the breakdown voltage increases, as seen in Figures 6 and 7. The relationship between the breakdown voltage and electric potential to the gap distance can be seen in Equation 5.

$$E = f \times \frac{v}{d} \tag{5}$$

where  $E$  is the electric field,  $f$  is the electric field non-uniformity factor,  $v$  is the breakdown voltage, and gap separation is represented by variable  $d$ .

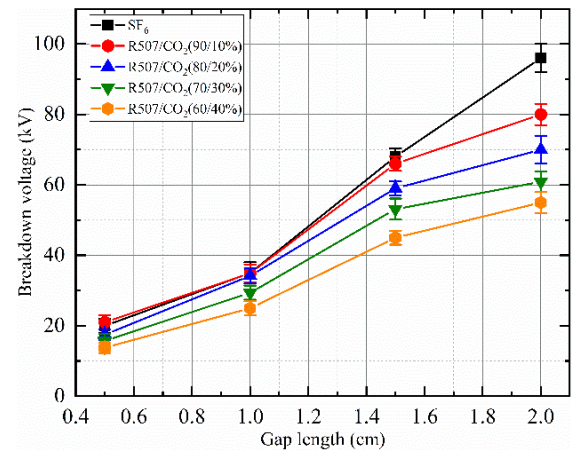
The R507 gas mixture exhibited comparable performance to SF<sub>6</sub> under a Point-plane HVAC test setup, as shown in Figure 6. Noticeably, at 1.5 cm air gap, the R507/CO<sub>2</sub> mixture

(90/10%) with a field utilization factor of 0.08 exhibited nearly equivalent breakdown strength to SF<sub>6</sub>. In contrast, the R507/CO<sub>2</sub> mixture (80/20%) at a 1.5 cm air gap demonstrated 0.89 times lower dielectric strength than SF<sub>6</sub>. At an air gap below 1.5 cm, the R507/CO<sub>2</sub> (90/10%) mixture shows breakdown strength equal to SF<sub>6</sub>. On the other hand, the R507/N<sub>2</sub> gas mixture of both 80 and 90% reveals equivalent dielectric strength at and below a 1 cm gap distance. Hence, applying R507/N<sub>2</sub> at low voltage levels is suggested. The results showed that the breakdown voltage of the R507/CO<sub>2</sub> mixture surpassed that of pure R507 due to the synergistic effect achieved through the combination. Besides the synergistic effect from the results in Figure 6, it is observed that by increasing the content of R507 in the gas mixture, the breakdown voltage decreases for a higher proportion relative to the R507 gas mixture with CO<sub>2</sub>/N<sub>2</sub> mixture. It is due to the high attachment cross-section of R507 at low energies of 0-0.5eV. Hence, a small proportion of R507 can increase the attachment of low-energy electrons, resulting in a higher breakdown voltage value. Conversely, all other mixture compositions displayed dielectric strength inferior to SF<sub>6</sub> under identical test conditions.

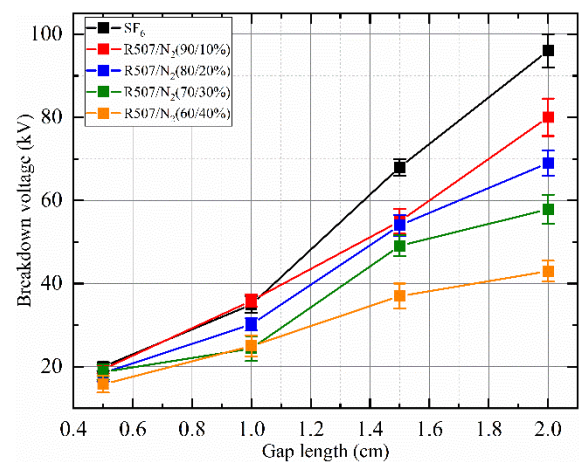
Figure 7 shows the influence of the R507/CO<sub>2</sub>/N<sub>2</sub> mixing ratio investigated under the point-plane configuration. The experimental results revealed for R507/CO<sub>2</sub> a discernible linear correlation between the breakdown voltage and the air gap up to a distance of 1.5 cm. Beyond this critical point, however, a pronounced and abrupt decrease in the insulation strength of the mixture relative to SF<sub>6</sub> was observed. Under the point-plane configuration, gas mixtures containing R507/CO<sub>2</sub> at compositions 90%/10% with a field utilization factor of 0.43 exhibited a superior dielectric strength, surpassing a maximum of 0.94 times to SF<sub>6</sub> at a 1 cm air gap. While the only R507/N<sub>2</sub>(90/10%) gas mixture shows equivalent dielectric strength to SF<sub>6</sub> at and below 1.2 cm of gap distance. It is observed that the R507/N<sub>2</sub>(90/10%) gas mixture at 1.8 cm has comparable results to SF<sub>6</sub> at a 1.5 cm gap distance. Consequently, these findings substantiate that R507 presents itself as a viable and environmentally advantageous alternative to SF<sub>6</sub> for medium voltage applications, given its remarkably minimized Global Warming Potential (GWP).

### C. LIGHTNING IMPULSE BREAKDOWN CHARACTERISTICS OF R507 GAS MIXTURE AT UNIFORM GAP DISTANCE

This investigation focuses on the R507 gas mixture lightning impulse breakdown characteristics with CO<sub>2</sub>/N<sub>2</sub>, considering different absolute pressure conditions. In compliance with ASTM D2477-07 and IEC60270 standard standards, a fixed air gap, represented as  $d$  of 0.5 mm, was maintained for the lightning impulse (LI) U50% testing. The pressure was then changed to within the range of 50 to 200 kPa. The gas dielectric strength and pressure are directly correlated. Pressure increases cause the electron's mean free path to condense, which lowers the electron's kinetic energy between collisions and potentially causes a reduction in ionization



(a)



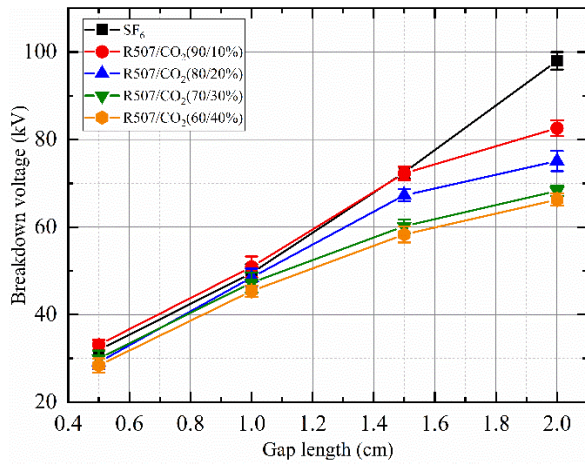
(b)

**FIGURE 6.** The HVAC breakdown voltage of point-plane electrodes at varying gap distances for (a) R507/CO<sub>2</sub> and (b) R507/N<sub>2</sub>.

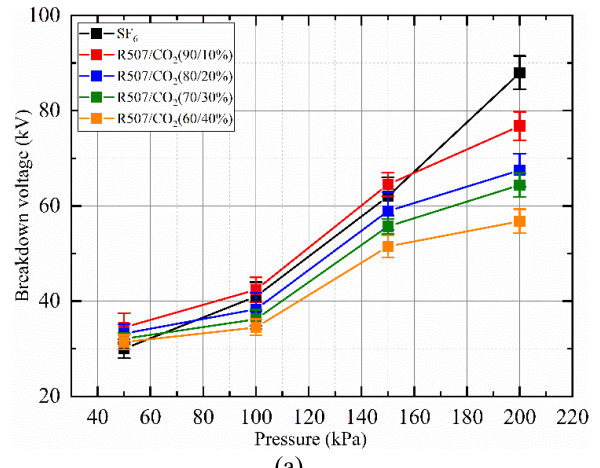
and an increase in breakdown voltage. Figure 8 shows the relationship between breakdown voltage and pressure.

As per the experimental data, the dielectric strength of the R507/CO<sub>2</sub> mixture rises with increasing pressure. Specifically, under a quasi-uniform electric field at 100 kPa, the R507/CO<sub>2</sub> mixture with a 90% R507 and 10% CO<sub>2</sub> composition yields 0.96 times higher dielectric strength than SF<sub>6</sub>. So, as the pressure rises above 100 kPa, SF<sub>6</sub> insulation strength shows a more noticeable improvement than the R507 gas mixture. In contrast, using a sphere-plane electrode design, the R507/N<sub>2</sub> gas mixture exhibits a lower breakdown voltage value than SF<sub>6</sub>. For the applied pressure range 50-200 kPa, the optimal mixture ratio containing 90% R507 gas with 10% CO<sub>2</sub> and N<sub>2</sub> gas mixture at 200 kPa shows 2.5 and 1.5 times, respectively, improved breakdown strength than its equivalent value at 50 kPa.

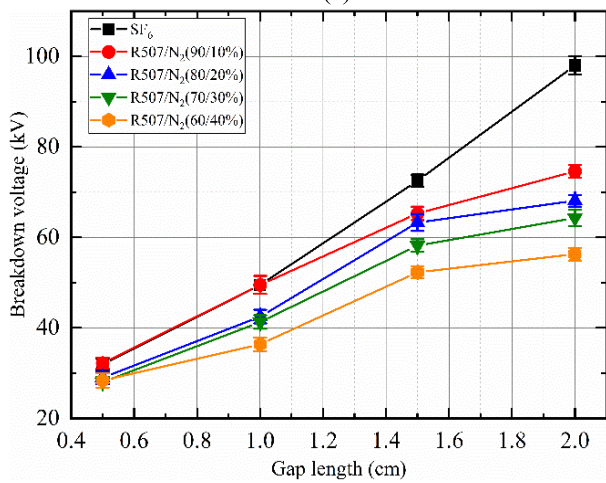
When considering the overall findings, the R507/CO<sub>2</sub> mixture exhibits encouraging prospects for use in medium-voltage applications. Notably, the mixture's dielectric strength reveals improvement as pressure rises. However,



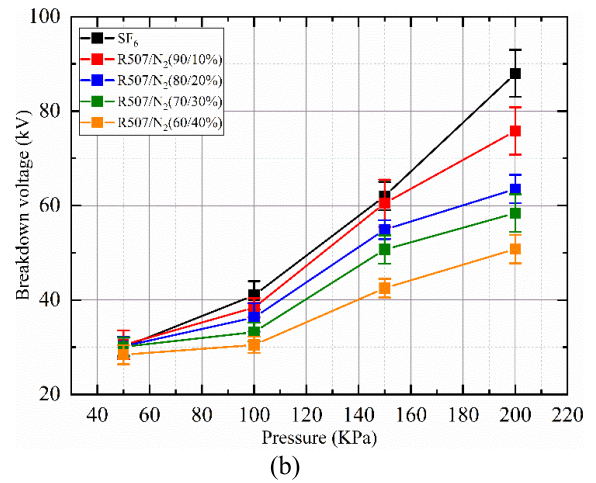
(a)



(a)



(b)



(b)

**FIGURE 7.** The HVAC breakdown voltage of Sphere-plane electrodes at varying gap distances for (a) R507/CO<sub>2</sub> and (b) R507/N<sub>2</sub>.

it does not outperform SF<sub>6</sub> at pressures higher than 150 kPa. These findings demonstrate the potential of the R507/CO<sub>2</sub> combination as a substitute in medium voltage applications, necessitating additional research and development for real GIS applications.

Likewise, LI U50 % experiments were performed to evaluate the behavior of the gas mixture for a highly non-uniform electric field. Figure 9 illustrates the nonlinear response that was found through investigation. Notably, at pressures higher than 1 kPa, a significant improvement in insulating strength was noted. The R507/CO<sub>2</sub> (90/10%) composition of all the investigated gas mixtures showed the best insulating strength. The breakdown strength of the R507/CO<sub>2</sub> (90/10%) mixture was 0.96 times greater than that of pure SF<sub>6</sub> gas. The breakdown voltages increase nonlinearly and beyond 160 kPa due to the non-homogeneous characteristics of the electric field; the SF<sub>6</sub> values are larger than all gas mixtures tested.

Moreover, further experimental investigation of breakdown voltages reveals that 90% R507/10% CO<sub>2</sub> under quasi and non-uniform electric fields at 180 kPa and 200 kPa are comparable to SF<sub>6</sub> at 150 kPa. It is observed that the optimal

**FIGURE 8.** Impulse breakdown under point-plane electrode settings at different pressures for (a) R507/CO<sub>2</sub> and (b) R507/N<sub>2</sub>.

composition of 90/10% of R507/CO<sub>2</sub> at around 220 kPa gives equivalent LI dielectric strength to SF<sub>6</sub> at 150 kPa under both quasi and non-uniform electric fields. The LI experimental results better understand the pressure variation versus the breakdown voltage characterization, as seen in Figure 9.

#### IV. R507 GAS MIXTURE INSULATION SELF-RECOVERABILITY ANALYSIS

A study at 150 MPa pressure and 5 mm gap separation was carried out to assess the insulator’s self-recoverability under high voltage alternating current (HVAC) conditions. To evaluate the gas insulator’s capacity to recover following each breakdown event, a set of 50 consecutive breakdown shots was performed. Figure 10 shows the measured mean breakdown voltage value of R507/CO<sub>2</sub> for the quasi-uniform electrode arrangement, which was 33.17 kV, with an exceptionally low standard deviation of 1.00217. The R507/CO<sub>2</sub> gas insulation self-recoverability properties for the non-uniform electric field design are carried out in the same experimental settings. With a standard deviation of 1.064, the R507/CO<sub>2</sub> mean breakdown voltage was measured as 21 kV. It is evident from Figure 10 that under a non-uniform electric field after



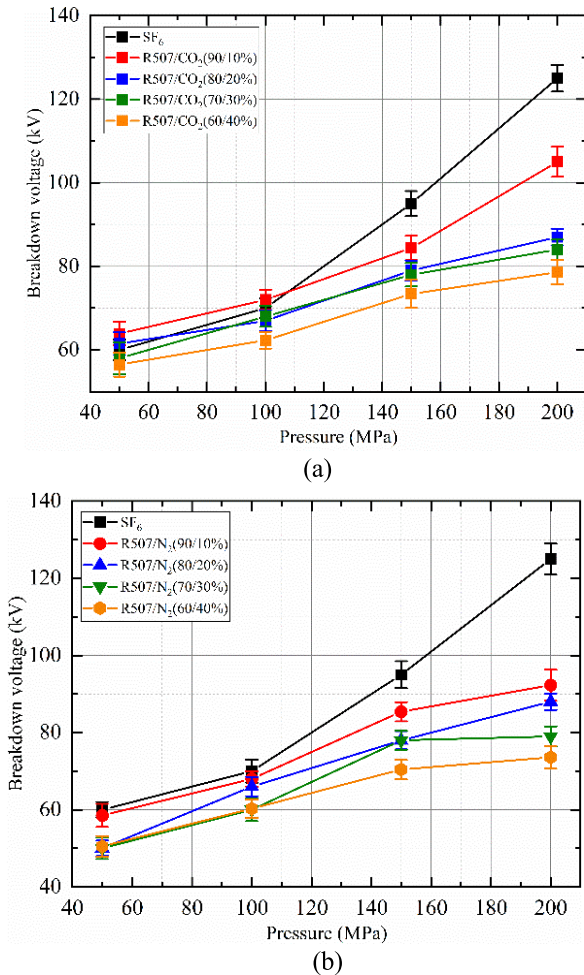


**FIGURE 9.** Impulse breakdown under sphere-plane electrode settings at different pressure for (a) R507/CO<sub>2</sub> and (b) R507/N<sub>2</sub>.

the 30<sup>th</sup> breakdown, the breakdown voltages of R507/CO<sub>2</sub> (90/10)% mixture show lower voltages than its mean breakdown voltage(21kV).

On the other hand, under a quasi-uniform electric field, it happens after the 45<sup>th</sup> breakdown shot. Hence, it is also concluded from this analysis that the proposed gas mixture at prolonged electric field stress and time will behave efficiently for a quasi-uniform electric field as compared to a non-uniform electric field.

These findings offer important new information on the insulator’s self-recoverability properties in HVAC settings. The close relationship between the average breakdown voltage values and the nominal voltage demonstrates the insulator’s effective recovery following each breakdown occurrence. The low standard deviations in both field configurations indicate the insulator’s reliable and consistent self-recovery capability.

**V. SYNERGISTIC EFFECT ANALYSIS OF R507 GAS MIXTURE**

HVAC breakdown experiments were conducted at 100 KPa in a quasi-uniform field to investigate the effect of the mixing

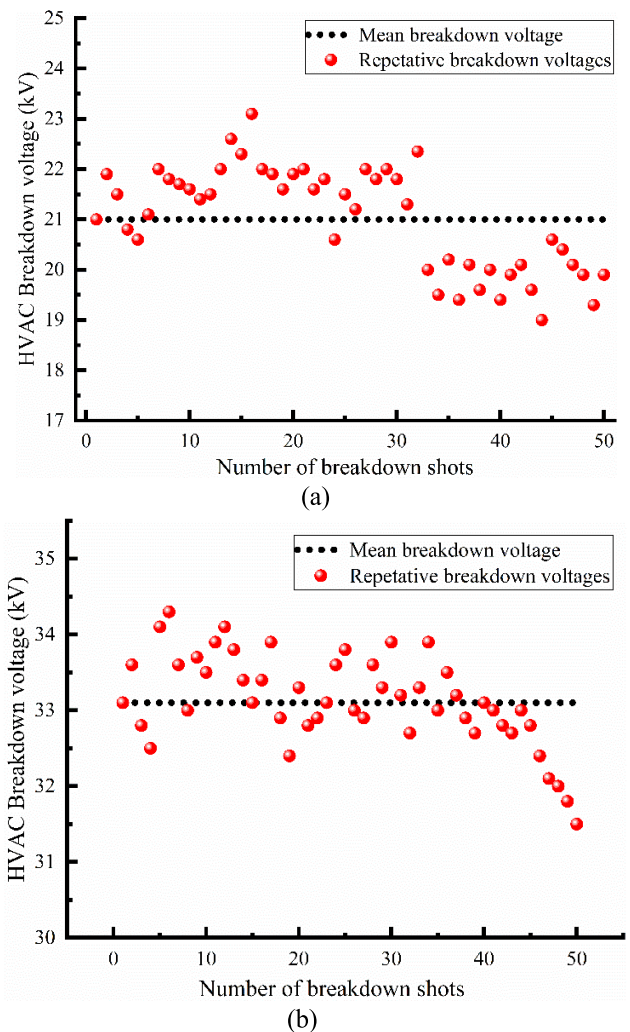


**FIGURE 10.** R507/CO<sub>2</sub> dielectric gas mixture self-recoverability analysis under HVAC test voltage for (a) non-uniform electric field and (b) quasi-uniform electric field.

ratio on the HFO-1336mzz(E) mixtures’ breakdown strength. The results are shown in Figure 11. It has been noted that when the base gas concentration rises, the breakdown voltage of the R507 gas mixture containing buffer gases also rises. Compared to all the other mixes tested, the R507/CO<sub>2</sub> mixture with a 90/10 % mixture concentration exhibits the highest dielectric strength value comparable to SF<sub>6</sub> gas. The key finding from this analysis is that the breakdown voltages of the R507 gas mixture are comparatively larger than those of the pure R507 gas, suggesting a synergistic action. In addition, the voltages of R507/CO<sub>2</sub> were higher than those of R507/N<sub>2</sub>. Hence, it can be proposed that R507 has a decent synergistic ability when mixed with buffer gas CO<sub>2</sub>.

Hence, the synergistic effect has been further studied by utilizing Equation 6 to evaluate the gas mixture’s non-linear breakdown voltage properties in the proposed gas mixture. The test results reveal that mixing R507 with CO<sub>2</sub> and N<sub>2</sub> results in varied dielectric performance. Therefore, examining how both mixed gaseous mediums work together is



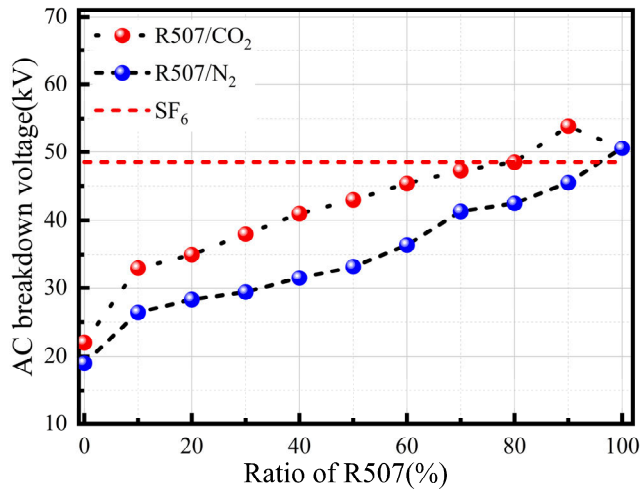


FIGURE 11. AC breakdown characteristics Sphere-plane of R507 gas mixture (P=100 kPa).

essential. The equation takes into account the breakdown voltage of  $V_{buffer}$  at their highest content under pressures ranging from 50 to 200 kPa, as determined through tests.

$$V_{mix} = V_{buffer} + \frac{m(V_{base} - V_{buffer})}{m + (1 - m)S} \quad V_{base} > V_{buffer} \quad (6)$$

$S$  in the equation denotes a synergistic coefficient whose value is ( $0 < S < 1$ ). The coefficient is defined as the measure of non-linearity in breakdown voltages of gas mixtures. When the  $S = 1$  for a given mixture, its breakdown voltage linearly increases with an increase in base and buffer gases' breakdown voltage. If  $S=0$ , then the gas mixture is made up exclusively of base gas ( $V_{mix} = V_{mixbuffer}$ ). When the  $S$  value lies between 0 and 1, the mixture breakdown voltage will non-linearly increase with breakdown voltages of base and buffer gases. Therefore, it should be noted that the smaller the value of  $S$  enhanced the synergistic effect.

For a certain mixing ratio and pressure range, a smaller value near zero indicates a positive favorable synergic effect, meaning the gas mixture is more suited for use as a dielectric medium. Particularly in the medium-pressure region of 100 to 200 kPa, the mix of R507/CO<sub>2</sub> gas (90/10 percent) functions relatively well. The value of  $S$  for R507 gas mixed with CO<sub>2</sub>/N<sub>2</sub> is represented in Figure 12 below. Figure 13 indicates that under HVAC voltage, the gas mixture at 150kPa has a lower  $S$  value than the corresponding R507/N<sub>2</sub> gas mixture. It is also observed that with the lower mixing ratio of R507, the coefficient  $S$  value is greater, and as the mixing ratio of base gas increases, the  $S$  value decreases. The lower  $S$  value for CO<sub>2</sub> indicates a positive favorable synergistic effect than N<sub>2</sub>. Hence, it is concluded that CO<sub>2</sub> is a better buffer gas to add to the R507 base gas.

Figure 13 below shows the  $S$  value for R507/CO<sub>2</sub> and R507/N<sub>2</sub> for pressure ranges from 50-200 kPa and the mixing ratio of base gas ranging from 60-90% in the mixture. The results showed that the synergistic effect of the R507/CO<sub>2</sub> mixture is lower than that of R507/N<sub>2</sub> for all the experimental

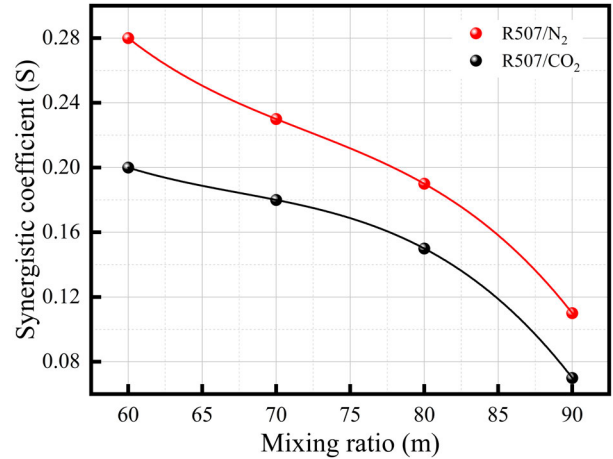


FIGURE 12. Synergistic analysis of R507 gas mixture.

conditions. In the case of R507/CO<sub>2</sub>, the optimal mixture composition, i.e. (90/10 %), shows the  $S$  coefficient value close to zero, indicating a positive synergistic effect for all pressure ranges. Moreover, the R507/CO<sub>2</sub>  $S$  values are 0 to 0.18, while the R507/N<sub>2</sub> values range from  $-0.3$  to 0.23.

Thus, synergistic effect analysis confirms that although the dielectric strengths of the buffer gases are nearly equal when tested alone, in a mixture with R507, the dielectric breakdown strength of R507/N<sub>2</sub> is lower than that of R507/CO<sub>2</sub> mixtures.

## VI. INFLUENCE OF ELECTRIC FIELD VARIATION ON INSULATION STRENGTH OF R507 GAS MIXTURE

An electric field sensitivity parameter, denoted as ' $K$ ,' is added to assess the difference between SF<sub>6</sub> and the R507/CO<sub>2</sub> gas mixture since it is imperative to investigate the sensitivity of the suggested gas to the applied electric field. Equation 7 defines the parameter as the extent to which a gas's insulation performance is degraded in a highly non-uniform electric field compared to a uniform electric field.

$$K = \frac{V_q - V_n}{V_q} \quad (7)$$

Here, the non-uniform field is represented by  $V_n$ , and the breakdown voltage of the quasi-uniform electric field is represented by  $V_q$ . The degree of inhomogeneities is indicated by  $K$  values; the higher the  $K$  value, the more sensitive the gas is to the applied electric field. Figure 14 displays the variation of  $K$  value with gas pressure for SF<sub>6</sub> and R507CO<sub>2</sub> gas mixes.

Figure 14 shows that the R507/CO<sub>2</sub> mixture has a lower  $K$  value than SF<sub>6</sub> at a pressure below 120 kPa. The sensitivity to the electric field increases with the amount of R507 gas concentration in the mixture. At 150 kPa absolute pressure, the R507 gas mixture with a composition of 90%,80%, and 70% shows the highest  $K$  value. The SF<sub>6</sub>  $K$  value is rising at a nearly steady pace, and at 150 kPa, it surpasses the entire R507/CO<sub>2</sub> gas mixture composition, indicating a greater sensitivity to the electric field. As a result, it was determined from the analysis that, relative to SF<sub>6</sub>, the R507/CO<sub>2</sub> gas mixture is less sensitive to the external electric field at pressures below

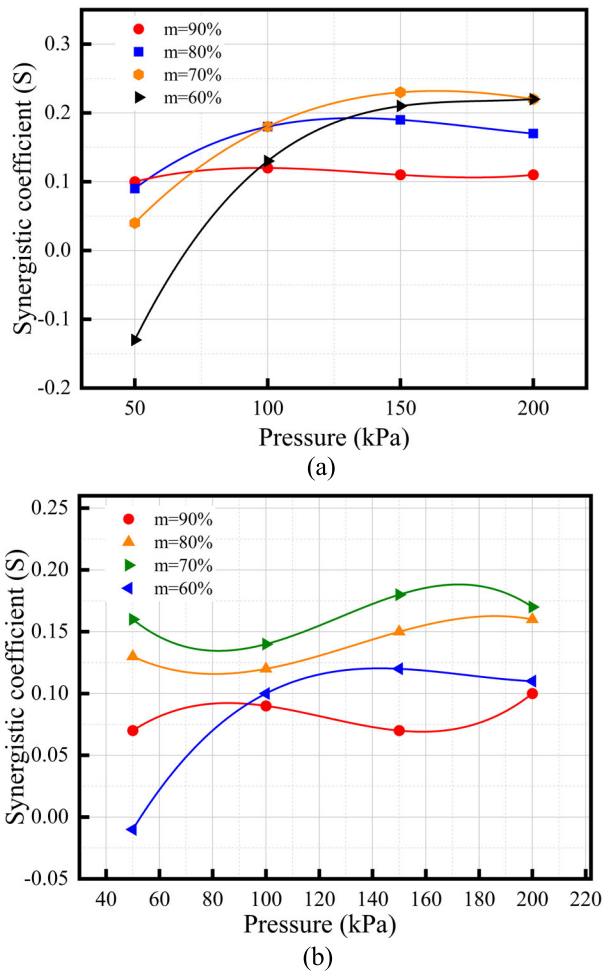


FIGURE 13. Synergistic effect of (a) R507/CO<sub>2</sub> (b) R507/N<sub>2</sub> gas mixtures.

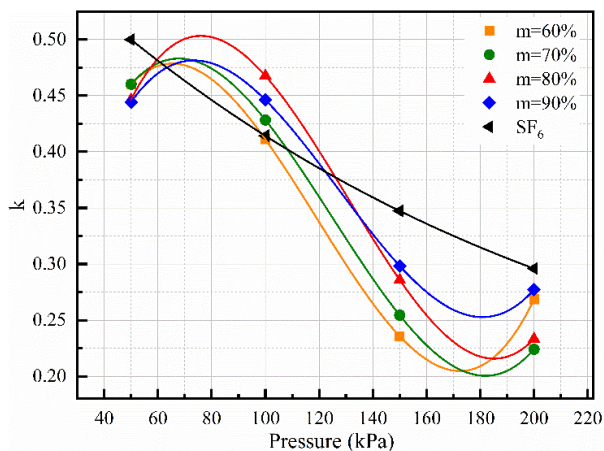


FIGURE 14. Influence of electric field inhomogeneity for R507/CO<sub>2</sub> gas mixture.

150 kPa. Consequently, at pressures lower than 150 kPa, the R507/CO<sub>2</sub> gas mixture has fascinating application possibilities and has a stronger insulating performance adjustment to the electric field than SF<sub>6</sub>.

Furthermore, to analyze the effect of different buffer gas mixtures with R507 gas, a variable  $R_b$  is introduced.  $R_b$  is

the ratio of the R507 gas mixture to the SF<sub>6</sub> gas under the same experimental conditions. The HVAC test setup under a quasi-uniform electric field is utilized here with a gap separation of 5 mm and varying absolute pressures from 50-200 kPa. The optimal gas mixture proportion of 90% R507 and 10% of CO<sub>2</sub> and N<sub>2</sub> is used for comparison purposes with SF<sub>6</sub>. Equation 8 demonstrates the calculation parameters.

$$R_b = \frac{R507_{AC}}{SF6_{AC}} \quad (8)$$

Figure 15 illustrates the  $R_b$  Curve variation at different pressure ranges and buffer gas compositions in relation to SF<sub>6</sub>. The breakdown voltage ratio of R507 gas with SF<sub>6</sub> exhibits a declining trend with rising pressure above 120 kPa. It can be seen that all pressure ranges R507/CO<sub>2</sub> have higher breakdown strength than the R507/N<sub>2</sub> gas mixture, except at 150 kPa, where both gases show almost equivalent dielectric strength. Beyond 150 kPa, the R507/CO<sub>2</sub> mixture again reveals higher insulation strength than its counterpart. Thus, this investigation indicates that the R507/CO<sub>2</sub> mixture exhibits a greater dielectric strength value than SF<sub>6</sub> at medium-pressure voltage ranges, specifically at or below 120 kPa.

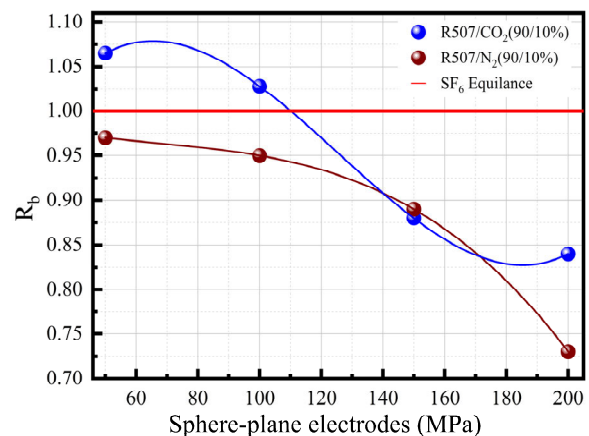


FIGURE 15. Relative breakdown strength of proposed gases to SF<sub>6</sub>.

## VII. GLOBAL WARMING POTENTIAL CHARACTERIZATION OF R507

Global warming potential is a critical parameter to be defined before suggesting gaseous dielectrics. The high GWP of SF<sub>6</sub> (23,500 times CO<sub>2</sub>) is the primary issue for researchers worldwide in finding an alternative. Equation 9 illustrates how the GWP is calculated using the environmental protection viewpoint and ideal gas conditions by adding the weight fractions of each component and multiplying that amount by the corresponding GWP [19]. The GWP value of R507 and the gas mixture with CO<sub>2</sub> and N<sub>2</sub> are shown in Figure 16. It is evident from the figure that the GWP of the R507/CO<sub>2</sub> mixture is lower than the R507/N<sub>2</sub> mixture. When the Gas content of R507 in the R507/CO<sub>2</sub> mixture is 10 %, it shows a smaller value of 1.6 times than the R507/N<sub>2</sub> mixture, and it is only 3.34 % of SF<sub>6</sub>. Therefore, using a gas mixture of R507

and CO<sub>2</sub> can significantly lessen the greenhouse impact.

$$GWP = \frac{k \times 3985 \times 99 + (1 - k) \times 44 \times 1}{k \times 3985 + (1 - k) \times 44} \quad (9)$$

where  $k$  represents the mixing ratio of base gas, GWP, and molar mass of R507 is 3985 and 99. Similarly, the GWP and molar mass of CO<sub>2</sub> are 1 and 44, and the GWP and molar mass of N<sub>2</sub> are 265 and 28, respectively.

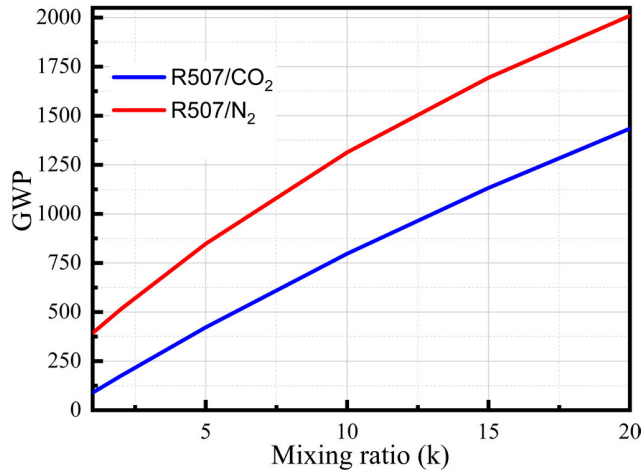


FIGURE 16. Global warming potential values with different mixing ratios.

Here, the mixing ratio of base gas is represented by variable  $k$ . The base gas R507 global warming potential is 3985 grams of carbon dioxide equivalent per kilogram (g-CO<sub>2</sub> eq/kg), and the molar mass is 99 grams/mol. Similarly, the GWP and molar mass of CO<sub>2</sub> and N<sub>2</sub> are 1, 265 (g-CO<sub>2</sub> eq/kg) and 44, 28 (g/mol), respectively.

### VIII. CONCLUSION

This study presented a comprehensive analysis of R507 HVAC and +LI voltage breakdown properties as well as its mixtures with CO<sub>2</sub> and N<sub>2</sub> as an environmentally suitable substitute to SF<sub>6</sub> for gas-insulated switchgear (GIS). Under various electric fields ranging from quasi-uniform to non-uniform, the effect of mixture ratio and gas pressure on the dielectric performance of the proposed gas mixture is examined and simultaneously compared with the hazardous SF<sub>6</sub> gas. Relevant results were obtained as follows.

- (1) The findings indicate that the proposed gas exhibits full SF<sub>6</sub> dielectric performance equivalency at a pressure of 150 kPa and an air gap of 1.5 cm; above these conditions, its insulating capabilities are scaled back compared to SF<sub>6</sub>. These results imply that R507/CO<sub>2</sub> at a 90:10 mixing ratio has successfully qualified to meet the requirements set by the IEC60010 standard for medium voltage GIS applications.
- (2) Positive synergistic effects between R507 and CO<sub>2</sub> gas are evident in comparison to R507-N<sub>2</sub> mixture. The mixing ratio and gas pressure arrangement are critical. In a combined analysis of the gas mixture's liquefaction temperature and power frequency breakdown characteristics, the 90% R507/ 10% CO<sub>2</sub> mixture suits the

minimum operating conditions in medium voltage GIS applications.

- (3) The optimal gas mixture comprising 90% R507/ 10% CO<sub>2</sub> also reveals a reduction of 80% in GWP value and reaches 95% of SF<sub>6</sub> insulation strength.

### REFERENCES

- [1] R. Arora and W. Mosch, *High Voltage and Electrical Insulation Engineering*. Hoboken, NJ, USA: Wiley, 2022.
- [2] US Environmental Protection Agency (USEPA), *Global Mitigation of Non-CO<sub>2</sub> Greenhouse Gases: 2010–2030*, USEPA, Washington, DC, USA, 2013.
- [3] C. Breidenich, D. Magraw, and A. Rowley, "The Kyoto Protocol to the United Nations framework convention on climate change," *Amer. J. Int. Law*, vol. 92, no. 2, pp. 315–331, 1998.
- [4] J. G. Owens, "Greenhouse gas emission reductions through the use of a sustainable alternative to SF<sub>6</sub>," in *Proc. IEEE Elect. Insul. Conf. (EIC)*, Jun. 2016, pp. 535–538.
- [5] L. G. Christophorou, J. K. Olthoff, and R. J. Van Brunt, "Sulfur hexafluoride and the electric power industry," *IEEE Elect. Insul. Mag.*, vol. 13, no. 5, pp. 20–24, Sep./Oct. 1997.
- [6] Y. Zhang, X. Zhang, Y. Li, Y. Li, Q. Chen, G. Zhang, S. Xiao, and J. Tang, "AC breakdown and decomposition characteristics of environmental friendly gas C<sub>5</sub>F<sub>10</sub>O/air and C<sub>5</sub>F<sub>10</sub>O/N<sub>2</sub>," *IEEE Access*, vol. 7, pp. 73954–73960, 2019.
- [7] R. Ahmed, R. A. Rahman, M. S. Kamarudin, M. F. M. Yousof, H. B. Ahmad, and A. A. Salem, "Feasibility of fluoronitrile (C<sub>4</sub>F<sub>7</sub>N) as a substitute to sulphur hexafluoride (SF<sub>6</sub>) in gas insulated application: A review," in *Proc. IEEE Int. Conf. Power Energy (PECon)*, Dec. 2022, pp. 391–396.
- [8] A. Beroual and A. Haddad, "Recent advances in the quest for a new insulation gas with a low impact on the environment to replace sulfur hexafluoride (SF<sub>6</sub>) gas in high-voltage power network applications," *Energies*, vol. 10, no. 8, p. 1216, 2017.
- [9] M. Rabie and C. M. Franck, "Computational screening of new high voltage insulation gases with low global warming potential," *IEEE Trans. Dielectr. Electr. Insul.*, vol. 22, no. 1, pp. 296–302, Feb. 2015.
- [10] H. S. Kharal, R. Ullah, Z. Ullah, R. Asghar, W. Uddin, B. Azeem, S. M. Ali, A. Haider, and M. Kamran, "Insulation characteristic of CCl<sub>2</sub>F<sub>2</sub> with mixtures of CO<sub>2</sub>/N<sub>2</sub> as a possible alternative to SF<sub>6</sub> substitute gas for high voltage Equipment's," in *Proc. Int. Conf. Power Gener. Syst. Renew. Energy Technol. (PGSRET)*, Sep. 2018, pp. 1–5.
- [11] Y. Li, S. Tian, L. Zhong, G. Chen, S. Xiao, Y. Cressault, Y. Fu, Y. Zheng, C. Preve, Z. Cui, Y. Zhang, F. Ye, D. Piccoz, G. Wang, Y. Li, Y. Tu, W. Zhou, J. Tang, and X. Zhang, "Eco-friendly gas insulating medium for next-generation SF<sub>6</sub>-free equipment," *iEnergy*, vol. 2, no. 1, pp. 14–42, Mar. 2023.
- [12] S. Hu, R. Qiu, and W. Zhou, "Dielectric properties and synergistic effect evaluation method of C<sub>4</sub>F<sub>7</sub>N mixtures," *IEEE Trans. Dielectr. Electr. Insul.*, early access, Sep. 18, 2023, doi: 10.1109/TDEI.2023.3316632.
- [13] R. Ahmad, R. A. Rahman, A. A. Salem, N. A. M. Jamail, A. A. Rahman, and H. A. Hamid, "Finite element analysis of electric field distribution in C<sub>4</sub>F<sub>7</sub>N as an alternative to SF<sub>6</sub> for electrical insulation," in *Proc. 3rd Int. Conf. High Voltage Eng. Power Syst. (ICHVEPS)*, Oct. 2021, pp. 126–131.
- [14] A. A. Salem, R. Abd-Rahman, M. S. Kamarudin, H. Ahmed, N. A. M. Jamail, N. A. Othman, M. F. M. Yousof, M. T. Ishak, and S. Al-Ameri, "The effect of insulator geometrical profile on electric field distributions," *Indones. J. Electr. Eng. Comput. Sci.*, vol. 14, no. 2, pp. 618–627, 2019.
- [15] Z. Gao, Y. Wang, S. Wang, R. Peng, W. Zhou, P. Yu, and Y. Luo, "Investigation of synthesis and dielectric properties of cC<sub>4</sub>F<sub>8</sub>O with its CO<sub>2</sub>/N<sub>2</sub> mixtures as SF<sub>6</sub> alternatives in gas-insulated applications," *IEEE Access*, vol. 8, pp. 3007–3015, 2019.
- [16] Z. Gao, Y. Luo, R. Peng, X. Wang, P. Yu, and W. Zhou, "Investigation on insulation properties of HFO-1336mzz(E) and N<sub>2</sub>/CO<sub>2</sub> mixtures as SF<sub>6</sub> substitutes in gas-insulated electrical applications," *High Voltage*, vol. 8, no. 1, pp. 48–58, Feb. 2023.
- [17] C. Ding, X. Hu, and Z. Gao, "Study on relative electrical strength of SF<sub>6</sub> substitute gas based on density functional theory," *IEEE Access*, vol. 10, pp. 75395–75403, 2022.



- [18] B. Khan, J. Saleem, F. Khan, G. Faraz, R. Ahmad, N. U. Rehman, and Z. Ahmad, "Analysis of the dielectric properties of R410A Gas as an alternative to SF<sub>6</sub> for high-voltage applications," *High Voltage*, vol. 4, no. 1, pp. 41–48, 2019.
- [19] R. Ullah, A. Rashid, A. Rashid, F. Khan, and A. Ali, "Dielectric characteristic of dichlorodifluoromethane (R12) gas and mixture with N<sub>2</sub>/air as an alternative to SF<sub>6</sub> gas," *High Voltage*, vol. 2, no. 3, pp. 205–210, 2017.
- [20] R. Ullah, Z. Ullah, A. Haider, S. Amin, and F. Khan, "Dielectric properties of tetrafluoroethane (R134) gas and its mixtures with N<sub>2</sub> and air as a sustainable alternative to SF<sub>6</sub> in high voltage applications," *Electr. Power Syst. Res.*, vol. 163, pp. 532–537, Oct. 2018.
- [21] M. Z. Saleem, M. Kamran, S. Amin, and R. Ullah, "Investigation on dielectric properties of chlorodifluoromethane and mixture with other N<sub>2</sub>/CO<sub>2</sub>/air as a promising substitute to SF<sub>6</sub> in high voltage application," *Electr. Eng.*, vol. 102, no. 4, pp. 2341–2348, Dec. 2020.
- [22] S. Soulie, "Study of the dielectric properties of HFO gas, and its application to reduce the environmental impact of medium-voltage systems," Ph.D. dissertation, Univ. Grenoble Alpes, 2021.
- [23] A. Hösl, J. Pachin, E. Eguz, A. Chachereau, and C. M. Franck, "Positive synergy of SF<sub>6</sub> and HFO1234ze(E)," *IEEE Trans. Dielectr. Electr. Insul.*, vol. 27, no. 1, pp. 322–324, Feb. 2020.
- [24] M. Rabie and C. M. Franck, "Comparison of gases for electrical insulation: Fundamental concepts," *IEEE Trans. Dielectr. Electr. Insul.*, vol. 25, no. 2, pp. 649–656, Apr. 2018.
- [25] R. Ahmed, R. A. Rahman, A. S. Aldosary, B. Al-Ramadan, R. Ullah, and A. Jamal, "Analysis of the insulation characteristics of hexafluorobutene (C<sub>4</sub>H<sub>2</sub>F<sub>6</sub>) gas and mixture with CO<sub>2</sub>/N<sub>2</sub> as an alternative to SF<sub>6</sub> for medium-voltage applications," *Appl. Sci.*, vol. 13, no. 15, p. 8940, 2023.
- [26] U. V. Mardolcar, F. J. V. Santos, and C. A. N. de Castro, "Dielectric properties of alternative refrigerants: A review," in *Proc. IEEE Int. Conf. Dielectric Liquids*, Jun. 2005, pp. 433–436.
- [27] *Standard Test Method for Dielectric Breakdown Voltage and Dielectric Strength of Insulating Gases at Commercial Power Frequencies*, ASTM International, Standard D2477, Jul. 2012.
- [28] *High-Voltage Test Techniques: Partial Discharge Measurements*, Standard IEC-60270, 2000, pp. 13–31.



**RIZWAN AHMED** received the bachelor's degree in electrical power engineering from COMSATS University Islamabad, Attock Campus, Pakistan, in 2015, and the master's degree in electrical power engineering from COMSATS University Islamabad, Abbottabad Campus, Pakistan, in 2019. He is currently pursuing the Ph.D. degree in high voltage engineering with Universiti Tun Hussein Onn Malaysia (UTHM), Malaysia. He is a Graduate Research Assistant under an international grant with the High-Voltage Laboratory. His research interests include high-voltage insulation, dielectric materials, outdoor insulators, grounding systems, and material engineering. He is a Registered Engineer with Pakistan Engineering Council (PEC). He was a recipient of the IEEE Power and Energy Society Best Paper Awards, in 2022 and 2023.



**RAHISHAM ABD-RAHMAN** (Member, IEEE) received the M.Eng. degree in electrical and electronic and the Ph.D. degree in high voltage from Cardiff University, U.K., in 2008 and 2012, respectively. He is currently an Associate Professor with the Faculty of Electrical and Electronic Engineering, Universiti Tun Hussein Onn Malaysia (UTHM). His research interests include dielectric materials, outdoor insulators, and discharge phenomena. He is a Chartered Engineer of U.K. (C.Eng.) and a member of engineering institutions, such as IET (MIET), IEEE (MIEEE), and the Board of Engineers Malaysia (BEM).



**ZAHID ULLAH** (Graduate Student Member, IEEE) received the B.S. degree in electrical engineering from UET Peshawar, in 2014, and the M.S. degree in electrical engineering from COMSATS University Islamabad, Abbottabad Campus, Abbottabad, Pakistan, in 2017. He is currently pursuing the Ph.D. degree in electrical engineering with Politecnico di Milano, Italy. He is a Lecturer with UMT Lahore, Pakistan. His research interests include smart grids, energy management, HV insulation media, renewable energy systems, and ICTs for power systems.



**RAHMAT ULLAH** received the bachelor's and master's degrees in electrical engineering from COMSATS University Islamabad, Abbottabad Campus, and the Ph.D. degree from Ghulam Ishak Khan University, Pakistan. Currently, he is a Post-doctoral Researcher with Cardiff University, U.K. His research interests include high-voltage insulation and power system monitoring and protection.



**IRFAN SAMI** received the B.Sc. degree in electrical engineering from the University of Engineering and Technology Peshawar, Pakistan, in 2016, the M.Sc. degree in electrical engineering from COMSATS University Islamabad, Abbottabad Campus, Abbottabad, Pakistan, in 2019, and the Ph.D. degree in electrical engineering with Chung-Ang University, Seoul, South Korea. He is currently a Senior Researcher with the Typhoon HIL Asia Pacific Engineering Centre, Milim Syscon Company Ltd., South Korea. His research interests include applications of robust control theory to grid-connected renewable energy systems and integration, electric drives, and their implementation in HIL and CHIL systems. He received the President Award from Chung-Ang University for his research achievements.



**MOHD FAIROUZ MOHD YOUSOF** (Member, IEEE) received the B.Eng. and M.Eng. degrees from Universiti Teknologi Malaysia and the Ph.D. degree from The University of Queensland, Australia, in 2015. He was a Visiting Researcher with TNB Research, from 2018 to 2019. He has been a Principal Consultant with Xair Energy Sdn Bhd, since 2019. He is currently an Associate Professor with the Department of Electrical Power Engineering, Universiti Tun Hussein Onn Malaysia (UTHM). His research interests include condition-based monitoring and assessment of high-voltage equipment, specifically power transformers and rotating machines. He is also a Registered Member of the Board of Engineers Malaysia (BEM) and a member of the Malaysian Society for Engineering and Technology (MySET).

...